Organic & Biomolecular Chemistry

Accepted Manuscript

This article can be cited before page numbers have been issued, to do this please use: K. Rustler, M. Mickert, J. Nazet, R. Merkl, H. Gorris and B. Koenig, *Org. Biomol. Chem.*, 2018, DOI: 10.1039/C8OB02122H.

ROYAL SOCIETY OF CHEMISTRY

rsc.li/obc

View Article Online
DOI: 10.1039/C8OB02122H

Journal Name

ARTICLE

Development of Photoswitchable Inhibitors for β-D-Galactosidase

Karin Rustler,[a] Matthias J. Mickert, [b] Julian Nazet,[c] Rainer Merkl,[c] Hans H. Gorris,[b] and Burkhard König*[a]

Received 00th January 20xx,
Accepted 00th January 20xx

DOI: 10.1039/x0xx00000x

www.rsc.org/

Azobenzenes are of particular interest as a photochromic scaffold for biological applications because of their high fatigue resistance, their large geometrical change between extended (*trans*) and bent (*cis*) isomer, and their diverse synthetic accessibility. Despite their wide-spread use, there is no reported photochromic inhibitor of the well-investigated tetrameric enzyme β-D-galactosidase, which plays an important role for biochemistry and single molecule studies. Herein, we report the synthesis of photochromic competitive β-D-galactosidase inhibitors based on the molecular structure of 2-phenylethyl β-D-thiogalactoside (PETG) and 1-amino-1-deoxy-β-D-galactose (β-D-galactosylamine). The thermally highly stable PETG-based azobenzenes show excellent photochromic properties in polar solvents and moderate to high photostationary states (PSS). The optimized compound **37** is a strong competitive inhibitior of β-D-galactosidase from *E. coli* and its inhibition constant (K_i) changes between 60 nM and 290 nM upon irradiation with light. Additional docking experiments supported the observed structure-activity relationship.

Introduction

By incorporating photochromic scaffolds into the molecular structure of known bioactive compounds, photons can be used as orthogonal control element providing high spatiotemporal precision in a – depending on the applied wavelength – non-invasive manner without risking contamination of the studied sample.[1-5] In contrast to photolyzable moieties the reversible approach of photoswitches and the absence of a cleaved side-product is beneficial.[6-8] Introducing this photochromic tool into a bioactive target leads – upon irradiation with light – to a reversible toggling between two states, affecting geometry, polarity, and charge distribution.[1,7,9] A variety of such photoresponsive scaffolds has been investigated, including dithienylethenes (DTEs), fulgi(mi)des, and azobenzenes, which can be characterized by their distinct switching mechanism either based on a 6-π-electrocyclic rearrangement (cyclization/ring-opening: DTEs, fulgi(mi)des) or an *E-Z* double-bond photoisomerization (azobenzenes). Their thermal stability differs from bistable (P-type: DTEs, fulgi(mi)des) to a tunable thermal reversibility ranging from ns to years (T-type: azobenzenes).[1,3,5,10-12] After the first publication of azobenzene in the late 1960s for the photoregulation of the activity of chymotrypsin,[13] the applications for photoactive moieties expanded towards the reversible light-triggered control of receptors,[14-17] bacterial growth,[18] vision restoration,[19,20] the respiratory chain,[21] and enzymatic activity.[13,22-27] The homotetrameric enzyme β-D-galactosidase from *E. coli* catalyzes the hydrolysis of glycosidic bonds in β-D-galactosides.[28] β-D-galactosidase has been extensively investigated and several competitive inhibitors including 2-phenylethyl β-D-thiogalactoside (PETG)[32] and 1-amino-1-deoxy-β-D-galactose (galactosylamine)[33] have been developed. One of the strongest competitive inhibitors of β-D-galactosidase (K_i: 0.6 nM; tight binding inhibitor) based on a mannostatin derivative was developed by Greul *et al*.[36] More recently, the inhibition of β-galactosidase has been investigated on the single molecule level in so-called femtoliter arrays.[30,37] This method provides statistic information about the individual behaviour of enzyme molecules in a population. The substrate turnover of a single β-galactosidase molecule – observable by the generation of a fluorescent product - is interrupted if an inhibitor binds to the active site, and the turnover resumes when the inhibitor is released. From the intermittency of the substrate turnover, stochastic information on individual binding and unbinding events can be retrieved. While it has not been possible to exert any control over these random events so far, a photochromic inhibitor would allow for switching the activity of single enzyme molecules on and off on demand. By extending the PETG-benzene moiety, we have designed a photochromic β-D-galactosidase-inhibitor, whose inhibitory activity can be controlled by irradiation with light orthogonal to the fluorescent read-out system resorufin ($\lambda_{Ex/Em}$ = 574/589 nm).[31,32]

Azobenzenes form one of the largest and most studied classes of photochromic molecules. First described in 1834,[38] their photoinduced *cis-trans* isomerization, which is accompanied by a large geometrical change and a considerable change in

[a] Institute of Organic Chemistry, University of Regensburg, 93053 Regensburg, Germany. E-mail: burkhard.koenig@ur.de
[b] Institute of Analytical Chemistry, Chemo- and Biosensors, University of Regensburg, 93053 Regensburg, Germany
[c] Institute of Biophysics and Physical Biochemistry, University of Regensburg, 93053 Regensburg, Germany

†Electronic Supplementary Information (ESI) available: Detailed experimental procedures and analytical data are available. See DOI: 10.1039/x0xx00000x

polarity, was discovered one century later in 1937 by G. S. Hartley.[39] Back-switching to the thermodynamically more stable *trans*-isomer can be achieved by irradiation with light of a different wavelength or may proceed by thermal relaxation.[1,3,5] Benefiting from those properties, we aimed for a strong difference in inhibitory activity upon light-induced switching between the two isomers. In this work, we report the design, synthesis, photochromic characterization, and inhibitory performance of water-soluble photochromic competitive β-D-galactosidase inhibitors based on the known structures of PETG and galactosylamine (Scheme 1).

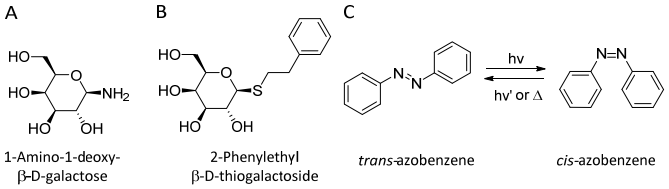

Scheme 1. Chemical structures of β-D-galactosidase inhibitors. (A) 1-Amino-1-deoxy-β-D-galactose (Galactosylamine).[33] (B) 2-Phenylethyl β-D-thiogalactoside (PETG).[32] (C) Photochromic azobenzene in its *trans*- and *cis*- isomeric state.

Results and Discussion

Design and synthesis of photochromic galactosylamine derivatives

Because of its high inhibitory activity, synthetic accessibility, and high reactivity at its C1 position for further functionalization, galactosylamine was chosen as one inhibitory scaffold for the introduction of a photoresponsive moiety. To attach the photoswitch azobenzene to the galactopyranoside moiety two different syntheses were conducted (Scheme 2). In a first synthetic attempt, D-galactose (**1**) was converted into its C1-amino derivative **2** (galactosylamine) in moderate yield upon reaction with ammonia in methanol for 48 hours at room temperature. Under these conditions the β-pyranose isomer was isolated as pure precipitate beside its α-pyranose and α/β-furanose form.[40] In the next step the β-pyranose product **2** was transformed into its photochromic amide **4** upon reaction with the carboxylic acid chloride azobenzene **3** in basic media in good yield; an acetone/water solvent mixture (5/1) allowed the solution of all reactants.[41] As compound **4** is based on a carboxy azobenzene core its photochromic properties are characterized by a long thermal half-life of its *cis*-isomer. To vary the photochromic properties (e.g. thermal half-life, absorption maxima), in addition, a second derivative, bearing an amino-azobenzene moiety directly attached to the galactosylamine, was synthesized. Compound **6** was obtained in a one-step reaction starting from D-galactose (**1**) and *para* aminoazobenzene **5**.[42] In analogy to the formation of β-D-galactosylamine **2** from D-galactose (**1**) again the β-pyranose form was isolated as major product.

Design of azobenzene-based PETG derivatives

Based on its benzene ring PETG was selected for azo-formation as the structural necessary modification is less drastic compared to the complete de novo introduction of an azobenzene and the risk to lose inhibitory activity consequently lower.

Synthesis of asymmetric azobenzene-based PETG derivatives

The asymmetric PETG-based azobenzene derivatives **34**-**42** were synthesized as outlined in Scheme 3. The general procedure is based on the transformation of the commercially available pentaacetylated β-D-galactose **7** into its C1-α-acetobromo-derivative **8** upon reaction with HBr in acetic acid.[43] In the next step, compound **8** was converted into its imino-methanamine salt **9** by reaction with thiourea and subsequently reduced to obtain the pentaacetylated β-D-thiogalactopyranoside **10**.[44] This thiosugar derivative was used for the reaction with differently bromo-substituted nitrobenzenes affording the corresponding pentaacetylated nitrobenzene β-D-thiogalactopyranosides **11**-**16**.[45] Besides the use of the native PETG moiety containing two CH_2 linking groups, the steric influence of linker length and substitution position was further investigated. Therefore, the employed bromo-substituted nitrobenzenes vary in their linker length (n = 0, 1, 2) and their substitution position (*ortho*, *para*). In order to perform a classical Mills reaction for the formation of an azo bridge, the nitro group was reduced to its amino function.[46] As reaction partner nitrosobenzene (**23**) and its sterically more demanding *para tert*-butyl substituted derivative **24**[47] were used affording the pentaacetylated β-D-thiogalactopyranoside azobenzenes **25**-**33** in low to moderate yields. Thereby, the *tert*-butyl group was installed to increase the steric demand upon light-induced *trans-cis* isomerization. For synthetic reasons, the *tert*-butyl substitution was placed in *para* position as the *ortho*-substituted nitrosobenzene showed no product formation in the Mills reaction due to steric hindrance. To regain the free hydroxy groups necessary for the interaction with the biological target the protected hydroxy groups were deacetylated in quantitative yield using potassium carbonate affording the desired photochromic thiogalactoside-based azobenzene derivatives **34**-**42**.[48]

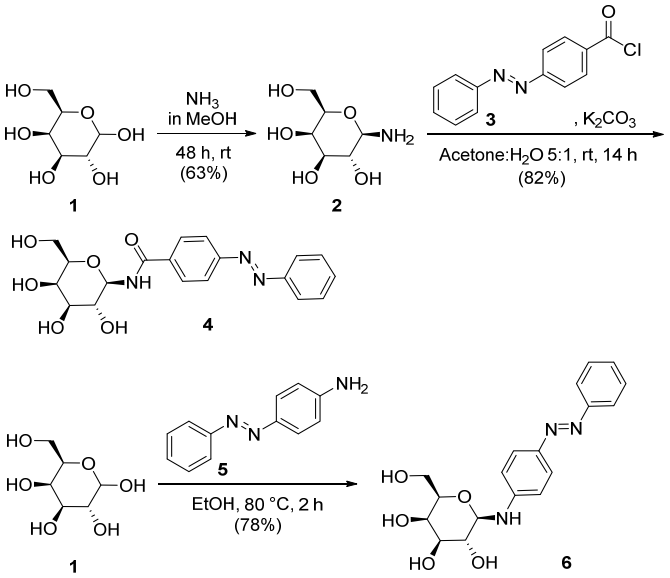

Scheme 2. Synthesis of azobenzene-based galactosylamine derivatives as competitive inhibitors for β-D-galactosidase (*Escherichia coli*).[40-42]

View Article Online
DOI: 10.1039/C8OB02122H

Journal Name

ARTICLE

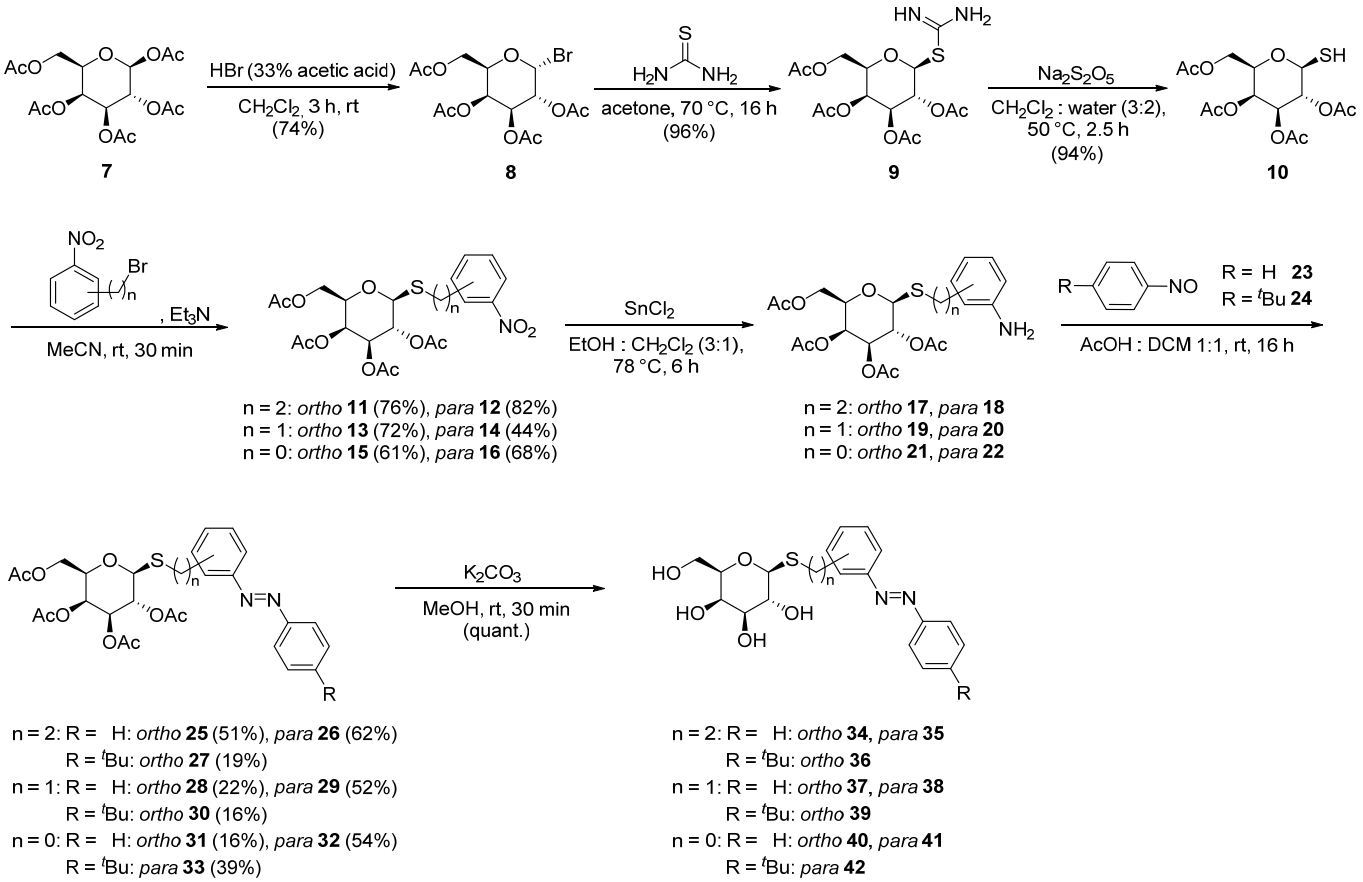

Scheme 3. Synthesis of asymmetric azobenzene-based PETG derivatives as competitive inhibitors for β-D-galactosidase (*E. coli*).[43-47]

Synthesis of the symmetric azobenzene-based PETG derivative

As design for a sterically more demanding inhibitor with increased binding probability a symmetrically phenethyl thiogalactopyranoside substituted azobenzene was synthesized. For the synthesis, a different synthetic strategy was used (Scheme 4). In a first step, the symmetric *para* hydroxyethyl substituted azobenzene **45** was synthesized. Therefore, commercially available *para* amino-phenethylalcohol **43** was converted into its nitroso derivative **44** via organoselenium-catalyzed oxidation by hydrogen peroxide.[49] The generated nitroso compound was subsequently reacted in a Mills reaction upon addition of amine **43** in acetic acid. The alcohol of the symmetric hydroxyethyl substituted azobenzene **45** was then converted to the bromide **46** using tetrabromomethane and triphenylphosphine. The thiol functional groups were introduced by reaction of **46** with thiourea followed by basic hydrolysis.[50] The glycosylation of thiol **47** with pentaacetylated galactopyranoside **7** under activation of the Lewis acid boron trifluoride etherate yielded the symmetrically glycosylated ethylazobenzene **48**. Deacetylation of the hydroxy protecting groups under basic conditions afforded the desired symmetrical target compound **49**.[48]

Photochromic properties

Photoisomerization studies of the competitive photochromic β-D-galactosidase inhibitors **4**, **6**, **34**-**42**, and **49** were conducted in phosphate buffer and DMSO, respectively, by absorption- and NMR-spectroscopy as well as HPLC-assisted analysis. Therefore, the dissolved compounds were irradiated with the indicated wavelengths to accumulate a substantial amount of their *cis*-isomer until the photostationary state (PSS) was reached. Thereby, the maximum representing the *trans*-isomer decreased and a new shoulder in the visible range, characteristic for the *cis*-isomer, evolved. For back isomerization the photochromic inhibitors were exposed to

visible light. The resulting isosbestic points in the absorption spectra indicate a clear two-component switching without any degradation or formation of a side product. For full UV-Vis absorption spectroscopic characterization see Figures S1-S12. In addition, the PSS was determined by HPLC and NMR measurements. The major photophysical properties of compounds **4**, **6**, **34**-**42**, and **49** are summarized in Table 1; for additional photochemical data see supplementary information Table S1-S3. All compounds showed excellent photochromic properties in DMSO, and phosphate buffer, respectively, with high photostationary states and fatigue resistance. Figure 1 shows exemplarily the UV-Vis absorption spectra (left) and the cycle performance (right) for the competitive β-D-galactosidase inhibitor **37** measured 50 µM in phosphate buffer + 0.1% DMSO. Black arrows indicate the characteristic changes in the absorption spectra upon irradiation with the indicated wavelengths. Dotted black arrows indicate isosbestic points.

The determination of the thermal half-lives (THL) of the *cis*-isomers of compounds **4**, **6**, **34**-**42**, and **49** was accomplished by monitoring the increase in absorbance which corresponds to the evolution of the *trans*-isomer. The data indicate slow thermal reversal of the *trans*-isomer at room temperature (except compound **6**), which is beneficial because constant irradiation during the enzymatic testing can be avoided.

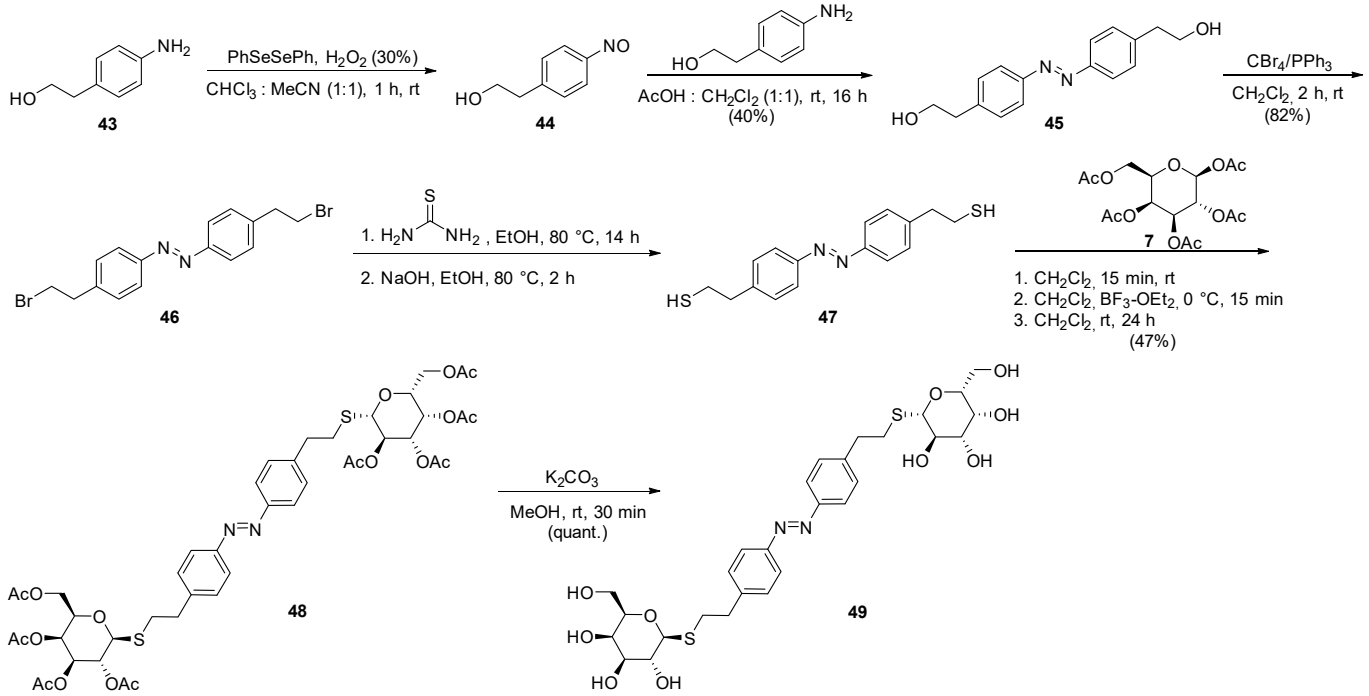

Scheme 4. Synthesis of the symmetric azobenzene-based PETG derivative as competitive inhibitor for β-D-galactosidase (*E. coli*).[48-50]

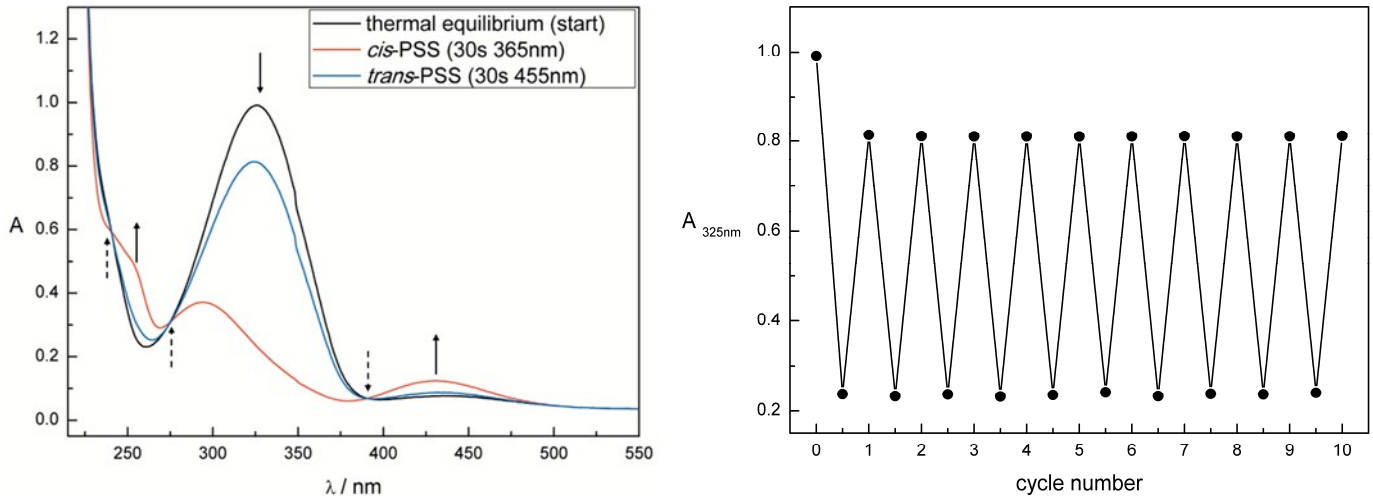

Figure 1. Photochromic properties of azobenzene-based PETG-derivative **37** (50 µM in phosphate buffer + 0.1% DMSO). Left. UV/Vis absorption spectra upon irradiation with λ = 365 nm until the *cis*-PSS is reached (30 s) and λ = 455 nm until the *trans*-PSS is reached (30 s). Black arrows indicate the characteristic changes in the absorption spectra upon switching. Dotted black arrows indicate isosbestic points. Right. Repetitive switching cycles after alternate irradiation with UV (λ = 365 nm) and blue (λ = 455 nm) light determined at 325 nm.

DOI: 10.1039/C8OB02132H

Table 1. Photochemical properties of azobenzene-based β-D-galactosidase inhibitors measured 50 µM in phosphate buffer + 0.1% DMSO, and 1% DMSO (labeled by *), respectively. [a] determined by analytical HPLC measurement of a preirradiated 50 µM solution at 20 °C. [b] determined by NMR-measurement of an irradiated sample in D_2O + 5% DMSO until the PSS was reached. n.d.: not detected due to fast thermal back relaxation.

Entry	Compound	λ_{max} *trans*-isomer [nm]	λ_{max} *cis*-isomer [nm]	Isosbestic points [nm]	THL	PSS-distribution
1	**4**	323	425	237, 280, 385	536 h	67% *cis* (375 nm)[a] 75% *trans* (405 nm)[a]
2	**6**	379	-	279, 293, 335, 464	1.69 s	n.d.
3	**34**	325	431	234, 274, 390	98.2 h	93% *cis* (365 nm)[b] 74% *trans* (455 nm)[b]
4	**35**	329	426	238, 278, 396	252 h	88% *cis* (365 nm)[a] 72% *trans* (455 nm)[a]
5	**36***	334	431	242, 287, 399	21.8 h	90% *cis* (365 nm)[b] 82% *trans* (455 nm)[b]
6	**37**	325	431	241, 275, 390	17.4 h	76% *cis* (365 nm)[b] 77% *trans* (455 nm)[b]
7	**38**	323	423	235, 273, 388	203 h	83% *cis* (365 nm)[a] 75% *trans* (455 nm)[a]
8	**39***	335	434	245, 288, 399	25.3 h	90% *cis* (365 nm)[b] 82% *trans* (455 nm)[b]
9	**40**	322	428	235, 254, 273, 428	262 h	81% *cis* (365 nm)[a] 63% *trans* (455 nm)[a]
10	**41**	348	429	238, 280, 421	94.3 h	88% *cis* (365 nm)[a] 69% *trans* (455 nm)[a]
11	**42***	352	433	241, 297, 432	37.0 h	90% *cis* (365 nm)[a] 76% *trans* (455 nm)[a]
12	**49**	338	430	240, 288, 407	104 h	93% *cis* (365 nm)[a] 74% *trans* (455 nm)[a]

Enzyme inhibition

Based on the determined relative inhibitory activity (see supplementary information Table S4) of the *trans*-isomer in its thermal equilibrium and the *cis*-isomer at its PSS of the competitive β-D-galactosidase inhibitors **4**, **6**, **34**-**42**, and **49**, the K_i values of the most promising derivatives were determined (Table 2).

Table 2. K_i [µM] values of photochromic competitive β-D-galactosidase inhibitors. K_i was determined by varying the inhibitor concentration at three different substrate concentrations (50, 100, and 150 µM). The standard deviation was calculated from the average of three independent measurements.

Entry	Compd.	K_i [µM] *trans*-isomer	K_i [µM] *cis*-PSS	Ratio (*cis*/*trans*)
1	**34**	0.7 ± 0.2	1.7 ± 0.5	2.4
2	**37**	**0.06 ± 0.01**	**0.29 ± 0.08**	**4.8**
3	**41**	62 ± 12	50 ± 11	1.2

From all tested photoswitchable inhibitors, the *ortho* substituted thiogalactosides with one (compound **37**) or two CH_2 spacers (compound **34**) between the sugar residue and the photochromic azobenzene part showed the strongest inhibition compared to the well-known inhibitor PETG, which has a K_i value of 7.2 µM.[34] Compared to PETG, the *trans*-isomer of compound **34** had a 10x lower K_i (0.7 µM) and the *trans*-isomer of compound **37** a 100x lower K_i (60 nM). Irradiating both inhibitors with 365 nm until the *cis*-PSS was reached allowed the accumulation of a substantial amount of the sterically more demanding isomer, which increased the K_i values of **34** to 1.7 µM (2.4x higher), of **37** to 0.29 µM (4.8x higher). The *trans*-isomer of the *para* substituted thiogalactosyl compound **41** without CH_2 spacer had a 10x higher K_i compared to PETG. Switching to the *cis*-PSS had almost no effect on K_i as indicated by a *cis*/*trans* ratio of around 1. β-D-galactosidase is a homotetramer comprising four identical active centers at the interface of two neighbouring subunits. The large binding pockets make it difficult to design photochromic derivatives with high *cis/trans* ratios. Comparing the inhibitors **34**, **37**, and **41**, compound **41** is the least sterically demanding inhibitor, which resulted in no activity change upon switching the molecule (K_i ratio 1.2; table 2). Changing the position of the azobenzene substitution from *para* (**41**) to *ortho* and extending the spacer length increased the *cis/trans* ratio by a factor of 2 for compound **34** (two CH_2 linking groups; ratio 2.4), and by a factor of 4 for compound **37** (one CH_2 linker; ratio 4.8). This implicates that the structural flexibility gained by one CH_2 group between sugar moiety and azobenzene (**37**) is sufficient for efficient binding into the enzyme's pocket.

Docking experiments

Compound **37** was docked to the β-D-galactosidase in its *trans*- and *cis*-isomeric state using VINA docking[51] as implemented in YASARA.[52] The best-ranked *cis*-isomer of **37** had an estimated

dissociation constant of 31 nM, whereas the estimated dissociation constant of its best-ranked *trans*-isomer is 27 nM, which supports a stronger binding of the *trans*-isomer. Figure 2 indicates that the sugar moiety of the ligand fits well into the binding pocket and fills it completely. The two aromatic rings of azobenzene, which are involved in light-induced switching are located at the surface of the protein and protrude out of the binding pocket. This localization argues against a drastic effect in inhibitory activity upon light-induced isomerization.

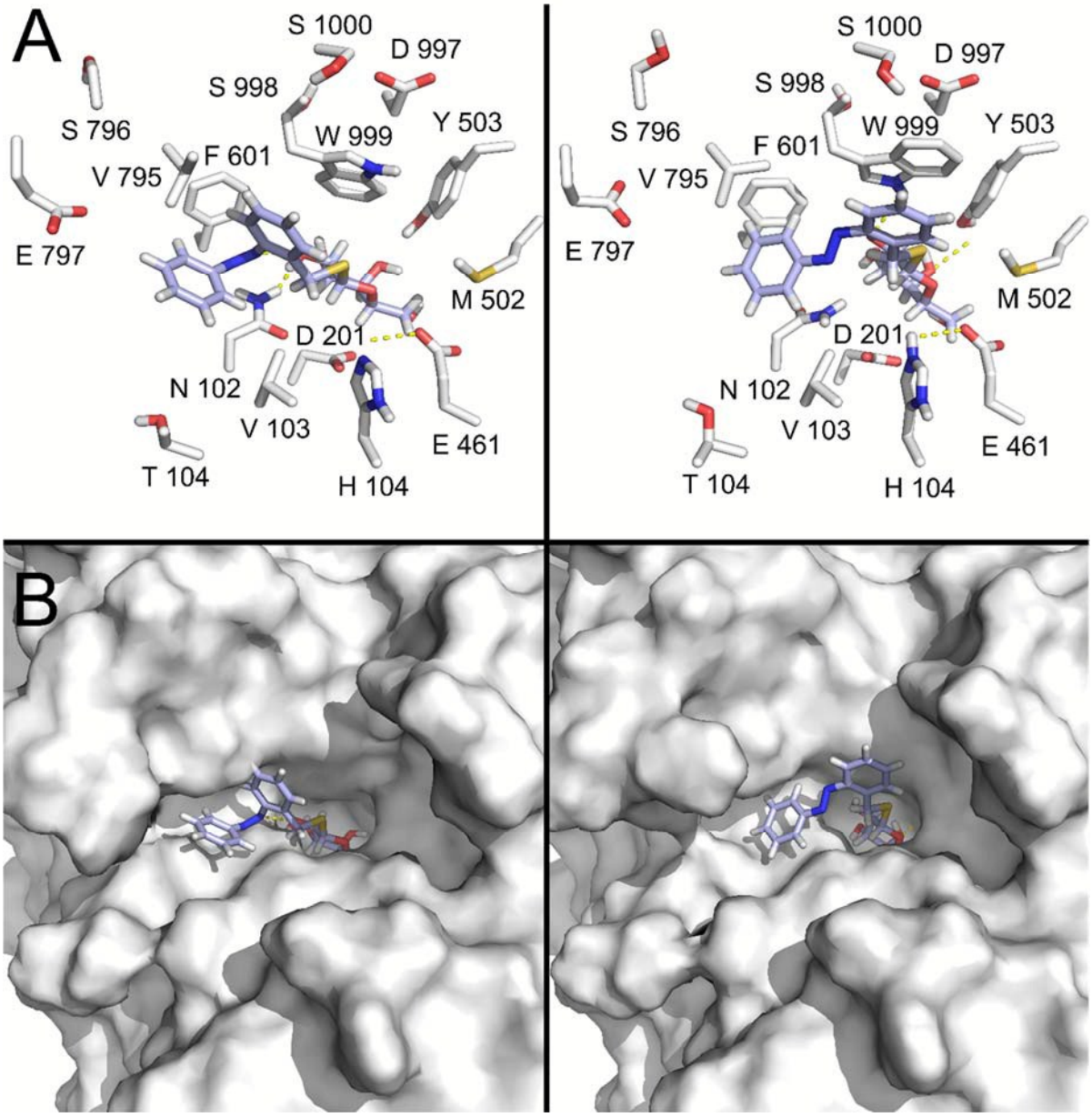

Figure 2. (A) A detailed view of the ligand **37** in its *cis*- (left panel) and *trans*-isomeric (right panel) state. The ligand is shown in blue; residues defined as flexible during docking are shown in white. Yellow dotted lines represent hydrogen bonds. (B) Surface view of the ligand in its *cis*- (left panel) and *trans*-isomeric (right panel) state.

Conclusion

In the presented work, we succeeded in the synthesis of thermally highly stable photochromic β-D-galactosidase inhibitors by modifying the chemical structure of potent inhibitors with an azobenzene moiety. All compounds show highly reversible photochromism in aqueous media with excellent fatigue resistance over ten measurement cycles. For the galactosylamine derivatives **4** and **6**, the high inhibitory activity of parent compound **2** (galactosylamine) could not be retained. In contrast, the PETG-based photochromic inhibitors **34**-**42** and **49** could be structurally optimized regarding their isomer-dependent activity by variation of their linker length, their substitution position, and their steric demand. Thereby, the photochromic moiety was first placed in *para* position to the inhibitory PETG moiety resulting in good inhibitory activity without significant isomer-dependent effect. To increase the effect of isomerization, the linker length was reduced resulting in a partial decrease of the inhibitory activity but no gain in

DOI: 10.1039/C8OB02122H

isomer specific effects. Therefore, the switching moiety was placed in *ortho* position increasing on one hand inhibitory activity and on the other hand isomer dependent effects. Compound **37** could be identified as a highly inhibitory active photochromic PETG-derivative with 5-fold difference upon switching and a K_i value of 60 nM (*trans*-isomer). However, the isomer-specific difference in activity has to be further improved before starting single molecule studies. Additional docking analysis explained the experimental observations.

Conflicts of interest

There are no conflicts to declare.

Acknowledgements

KR and BK thank the ERASynBio grant (MODULIGHTOR) (PCIN-2015-163-C02-01) for financial support. KR thanks Josef Kiermaier and Wolfgang Söllner for mass spectrometry analysis. HHG thanks the DFG for a Heisenberg Fellowship (grant GO 1968/5-1).

Notes and references

1 W. A. Velema, W. Szymanski, B. L. Feringa, *J. Am. Chem. Soc.*, 2014, **136**, 2178-2191.
2 D. Bléger and S. Hecht, *Angew. Chem. Int. Ed.,* 2015, **54**, 11338-11349.
3 W. Szymanski, J. M. Beierle, H. A. V. Kistemaker, W. A. Velema, B. L. Feringa, *Chem. Rev.,* 2013, **113**, 6114-6178.
4 M. M. Lerch, M. J. Hansen, G. M. van Dam, W. Szymanski, B. L. Feringa, *Angew. Chem. Int. Ed.,* 2016, **55**, 10987-10999.
5 C. Brieke, F. Rohrbach, A. Gottschalk, G. Mayer, A. Heckel, *Angew. Chem. Int. Ed.,* 2012, **51**, 8446-8476.
6 M. M. Lerch, M. J. Hansen, W. A. Velema, W. Szymanski, B. L. Feringa, *Nat. Commun.,* 2016, **7**, 12054.
7 H. Bouas-Laurent and H. Dürr, *Pure Appl. Chem.,* 2001, **73**, 639-665.
8 P. Klán, T. Šolomek, C. G. Bochet, A. Blanc, R. Givens, M. Rubina, V. Popik, A. Kostikov, J. Wirz, *Chem. Rev.,* 2013, **113**, 119-191.
9 M. M. Lerch, W. Szymanski, B. L. Feringa, *Chem. Soc. Rev.,* 2018, **47**, 1910-1937.
10 J. Garcia-Amorós, M. Díaz-Lobo, S. Nonell, D. Velasco, *Angew. Chem. Int. Ed.,* 2012, **51**, 12820-12823.
11 J. Garcia-Amorós, M. C. R. Castro, P. Coelho, M. M. M. Raposo, D. Velasco, *Chem. Commun.,* 2013, **49**, 11427-11429.
12 J. Garcia-Amorós, S. Nonell, D. Velasco, *Chem. Commun.,* 2012, **48**, 3421-3423.
13 H. Kaufman, S. M. Vratsanos, B. F. Erlanger, *Science,* 1968, **162**, 1487-1489.
14 W. J. Deal, B. F. Erlanger, D. Nachmansohn, *Proc. Natl. Acad. Sci. U. S. A.,* 1969, **64**, 1230-1234.
15 M. Volgraf, P. Gorostiza, R. Numano, R. H. Kramer, E. Y. Isacoff, D. Trauner, *Nat. Chem. Biol.,* 2006, **2**, 47-52.
16 P. Gorostiza, M. Volgraf, R. Numano, S. Szobota, D. Trauner, E. Y. Isacoff, *Proc. Natl. Acad. Sci. U. S. A.,* 2007, **104**, 10865-10870.
17 M. Volgraf, P. Gorostiza, S. Szobota, M. R. Helix, E. Y. Isacoff, D. Trauner, *J. Am. Chem. Soc.,* 2007, **129**, 260-261.
18 M. Wegener, M. J. Hansen, A. J. M. Driessen, W. Szymanski, B. L. Feringa, *J. Am. Chem. Soc.,* 2017, **139**, 17979-17986.
19 A. Polosukhina, J. Litt, I. Tochitsky, J. Nemargut, Y. Sychev, I. de Kouchkovsky, T. Huang, K. Borges, D. Trauner, R. N. van Gelder, R. H. Kramer, *Neuron,* 2012, **75**, 271-282.
20 I. Tochitsky, A. Polosukhina, V. E. Degtyar, N. Gallerani, C. M. Smith, A. Friedman, R. N. van Gelder, D. Trauner, D. Kaufer, R. H. Kramer, *Neuron,* 2014, **81**, 800-813.
21 N. A. Simeth, A. C. Kneuttinger, R. Sterner, B. König, *Chem. Sci.,* 2017, **8**, 6474-6483.
22 N. A. Simeth, L. M. Altmann, N. Wössner, E. Bauer, M. Jung, B. König, *J. Org. Chem.,* 2018, **83**, 7919-7927.
23 B. Eisel, F. Hartrampf, T. Meier, D. Trauner, *FEBS Lett.,* 2018, **592**, 343-355.
24 D. Wilson, J. W. Li, N. R. Branda, *ChemMedChem,* 2017, **12**, 284-287.
25 R. Ferreira, J. R. Nilsson, C. Solano, J. Andréasson, M. Grøtli, *Sci. Rep*., 2015, **5**, 9769-9776.
26 J. Broichhagen, I. Jurastow, K. Iwan, W. Kummer, D. Trauner, *Angew. Chem. Int. Ed.,* 2014, **53**, 7657-7660.
27 D. Wutz, D. Gluhaceic, A. Chakrabarti, K. Schmidtkunz, D. Robaa, F. Erdmann, C. Romier, W. Sippl, M. Jung, B. König, *Org. Biomol. Chem.,* 2017, **15**, 4882-4896.
28 D. H. Juers, B. W. Matthews, R. E. Huber, *Protein Science*, 2012, **21**, 1792-1807.
29 Q. Husain, *Crit. Rev. Biotechnol.,* 2010, **30**, 41-62.
30 P. Mogalisetti, H. H. Gorris, M. J. Rojek, D. R. Walt, *Chem. Sci.,* 2014, **5**, 4467-4473.
31 M. J. Mickert, H. H. Gorris, *J. Phys. Chem. B,* 2018, **122**, 5809-5819.
32 A. G. Hadd, D. E. Raymond, J. W. Halliwell, S. C. Jacobson, J. M. Ramsey, *Anal. Chem.,* 1997, **69**, 3407-3412.
33 R. E. Huber, M. T. Gaunt, *Can. J. Biochem.,* 1982, **60**, 608-612.
34 R. B. Liebherr, A. Hutterer, M. J. Mickert, F. C. Vogl, A. Beutner, A. Lechner, H. Hummel, H. H. Gorris, *Anal. Bioanal. Chem.,* 2015, **407**, 7443-7452.
35 M. Kleban, P. Hilgers, J. N. Greul, R. D. Kugler, J. Li, S. Picasso, P. Vogel, V. Jäger, *ChemBioChem,* 2001, **2**, 365-368.
36 J. N. Greul, M. Kleban, B. Schneider, S. Picasso, V. Jäger, *ChemBioChem,* 2001, **2**, 368-370.
37 H. H. Gorris, D. M. Rissin, D. R. Walt, *PNAS*, 2007, **104**, 17680-17685.
38 E. Mitscherlich, *Ann. Pharm.* **1834**, *12*, 311-314.
39 G. S. Hartley, *Nature* **1937**, *140*, 281-282.
40 L. Lindner, P. Klüfers, *Z. Anorg. Allg. Chem.,* 2015, **641**, 1869-1873.
41 M. P. Seed, M. Burnet, H. J. Gutcke, *Assignee Diosamine Development Corporation Patent,* 2008, **WO2008059003 A1**.
42 R. Rajaganesh, A. Gopal, T. M. Das, A. Ajayaghosh, *Org. Lett.,* 2012, **14**, 748-751.
43 A. G. Watts, T. Kantner, A. B. MacKenzie, *Assignee The University of Bath,* 2010, **WO2010070300A2**.
44 L. M. Doyle, S. O'Sullivan, C. Di Salvo, M. McKinney, P. McArdle, P. V. Murphy, *Org. Lett.,* 2017, **19**, 5802-5805.
45 X. Xiao, Y. Zhao, P. Shu, X. Zhao, Y. Liu, J. Sun, Q. Zhang, J. Zeng, Q. Wan, *J. Am. Chem. Soc.,* 2016, **138**, 13402-13407.
46 X. Li, L. Huang, X. Hu, X. Huang, *Org. Biomol. Chem.,* 2009, **7**, 117-127.
47 H. Wang, S. Sun, J. Cheng, *Tetrahedron Letters,* 2017, **58**, 3875-3878.
48 M. Poláková, S. Šesták, E. Lattová, L. Petruš, J. Mucha, I. Tvaroška, J. Kóňa, *Eur. J. Med. Chem.,* 2011, **46**, 944-952.
49 D. Zhao, M. Johansson, J.-E. Bäckvall, *Eur. J. Org. Chem.,* 2007, **26**, 4431-4436.
50 N. Marquestaut, A. Martin, D. Talaga, L. Servant, S. Ravaine, S. Reculusa, D. M. Bassani, E. Gillies, F. Lagugné-Labarthet, *Langmuir,* 2008, **24**, 11313-11321.
51 O. Trott, A. J. Olson, *J. Comput. Chem.,* 2010, **31**, 455-461.
52 E. Krieger, G. Vriend, *Bioinformatics,* 2014, **30**, 2981-2982.